JOURNAL OF BACTERIOLOGY, July 2006, p. 4654–4662 Vol. 188, No. 13
0021-9193/06/$08.00+0 doi:10.1128/JB.00120-06

In Vivo Dissection of the *Helicobacter pylori* Fur Regulatory Circuit by Genome-Wide Location Analysis†

Alberto Danielli,[1] Davide Roncarati,[1] Isabel Delany,[2] Valentina Chiarini,[1] Rino Rappuoli,[2] and Vincenzo Scarlato[1,2]*

Department of Biology, University of Bologna, Bologna, Italy,[1] and Molecular Immunology Unit, Chiron Vaccines, Siena, Italy[2]

Received 23 January 2006/Accepted 13 April 2006

Iron homeostasis is particularly important in pathogenic bacteria, which need to compete with the host for this essential cofactor. In *Helicobacter pylori*, a causative agent of several gastric pathologies, iron uptake and storage genes are regulated at the transcriptional level by the ferric uptake regulator Fur. The regulatory circuit of Fur has recently come under focus because of an intimate interlink with a broader regulatory network governing metal homeostasis, acidic response, and virulence. To dissect the Fur regulatory circuit and identify in vivo targets of regulation, we developed a genome-wide location analysis protocol which allowed the identification of 200 genomic loci bound by Fur as well as the investigation of the binding efficiency of the protein to these loci in response to iron. Comparative analysis with transcriptomes of wild-type and *fur* deletion mutant strains allowed the distinction between targets associated with Fur regulation and genes indirectly influenced by the *fur* mutation. The Fur regulon includes 59 genes, 25 of which appear to be positively regulated. A case study conducted by primer extension analysis of two oppositely regulated genes, *hpn2* and *flaB*, suggests that negative regulation as well as positive regulation occurs at the transcriptional level. Furthermore, the results revealed the existence of 13 Fur targeted loci within polycistronic operons, which were associated with transcript deregulation in the *fur* mutant strain. This study provides a systematic insight of Fur regulation at the genome-wide level in *H. pylori* and points to regulatory functions extending beyond the classical Fur repression paradigm.

Iron is of crucial importance in most organisms and particularly in bacterial pathogens, which have to compete with their hosts for this essential nutrient (29). In many bacteria, iron homeostasis is tightly regulated, and iron starvation triggers the expression of iron-scavenging systems and of virulence factors such as hemolysins and toxins (18). Like other gram-negative bacteria, *Helicobacter pylori*, a human pathogen associated with mild to severe stomach diseases, has adapted to cope with environmental fluctuations of iron availability. Several ferrous and ferric uptake systems, as well as iron-scavenging and iron storage genes, were discovered by determining the genome sequences of clinical isolates (1, 31). Interestingly, the concerted expression of several of these systems is transcriptionally regulated by the ferric uptake regulator Fur (10, 32).

Classical Fur regulation has been well documented for *Escherichia coli*, *Pseudomonas aeruginosa*, and *Bacillus subtilis* and proceeds through transcriptional repression mediated by concentrations of intracellular iron, which acts as a repressive cofactor (14, 33). Iron-dependent conformational changes of the protein alter its affinity for conserved AT-rich operators (Fur boxes) at regulated promoters (2, 13, 15) and influence the rate of transcriptional initiation. In a small number of cases, Fur has been reported to act positively rather than negatively in the expression of certain genes. Recently, the mechanism of positive regulation by Fur of a number of these genes has been elucidated as being indirect and taking place at the posttranscriptional level through the repression of an antisense regulatory RNA (23, 35). A similar posttranscriptional control mechanism in not known for *H. pylori*. However, in this pathogen Fur can directly regulate the transcription of both the iron-induced *pfr* gene and the iron-repressed *frpB1* gene (coding for a ferritin and an outer membrane protein, respectively), according to the iron status of the protein, through affinity variations for specific operators in their promoters (10).

Recently, iron-dependent regulation in *H. pylori* has received increased attention, because metal ion-dependent regulators, such as Fur and NikR, are involved with the acid resistance HP0166 ArsR regulator in a broader regulatory network, which governs the concerted expression of genes important for gastric colonization, urease among others (3, 28). Functional genomic studies indicated a pleiotropic role of Fur and NikR in transcription (4, 12, 21, 25) and revealed several genes which are possibly subject to coregulation. However, the existence of two regulators feeding into the same circuit complicates dissection of their regulatory network. In fact, direct regulatory roles and indirect effects remain elusive to distinguish. For example, NikR was proposed to influence indirectly the rate of iron-dependent Fur regulation by transcriptional regulation of a *tonB* operon, involved in iron uptake (4). Moreover, the decreased transcription of several genes in *fur* deletion strains was attributed to indirect effects, because this type of regulation is atypical for a postulated repressor (12). Finally, it has been shown recently that Fur and NikR may coregulate gene transcription by binding to separate as well as overlapping operators (6).

To begin dissection of the metal regulatory circuit in *H. pylori* and discriminate between direct and indirect Fur regu-

* Corresponding author. Mailing address: Department of Biology, University of Bologna, Via Selmi 3, 40126 Bologna, Italy. Phone: 39 051 209 4204. Fax: 39 051 209 4286. E-mail: vincenzo.scarlato@unibo.it.

† Supplemental material for this article may be found at http://jb.asm.org/.

lation, we implemented Fur chromatin immunoprecipitations, investigating at which sites the Fur protein binds to DNA in vivo by genome-wide location analyses. The results were compared with transcriptome analyses of wild-type (wt) and *fur* knockout strains and led to the identification of a set of genes subject to direct regulatory Fur control.

MATERIALS AND METHODS

Bacterial strains and growth conditions. *H. pylori* wild-type G27 and *fur* knockout (*fur*::*km*) strains were recovered from frozen stocks on Columbia agar plates containing 5% horse blood, 0.2% cyclodextrin, and Dent's or Skirrow's antibiotic supplement under microaerophilic conditions (Oxoid) for 2 to 3 days. After passage on fresh plates, bacteria were cultured in a 9% CO_2-91% air atmosphere. Liquid cultures of *H. pylori* were grown in modified *Brucella* broth containing Dent's or Skirrow's antibiotic supplement and 5% fetal calf serum. When required, kanamycin was added to a final concentration of 25 μg/ml. For iron response, 10 ml of *H. pylori* grown to an optical density at 600 nm (OD_{600}) of 0.6 to 1.1 in modified *Brucella* broth at 37°C with shaking was treated with 1 mM $FeSO_4$ (Fe^+) or 100 μM 2,2′-dipyridyl (Fe^-) for 15 min under microaerophilic conditions. A 15-min treatment was chosen to investigate an early Fur-dependent transcriptional response rather than a long-term adaptation to iron conditions.

Immunoblotting. One-milliliter aliquots of the same *H. pylori* culture were collected at regular time intervals during growth, ranging from an OD_{600} of 0.4 to an OD_{600} of 1.1, and resuspended in phosphate-buffered saline to an OD_{600} of 4, and total protein extracts from 10 μl of each sample were separated by sodium dodecyl sulfate-polyacrylamide gel electrophoresis (SDS-PAGE) and subjected to immunoblotting with Fur and NikR antisera as previously described (6).

Cross-linking and immunoprecipitation of Fur-DNA complexes (Fur-IP). Ten milliliters of *H. pylori* cultures was fixed with 1% formaldehyde at room temperature for 15 min under gentle agitation; thereafter, glycine was added (0.125 M) and samples were shaken for an additional 10 min. Cross-linked cells were pelleted by centrifugation, washed twice in 1 volume of cold phosphate-buffered saline, washed once in 150 mM NaCl, 10 mM Tris-HCl (pH 8.0), 10 mM EDTA (pH 8.0), and 0.25% Triton X-100, and resuspended in 2 ml TE (10 mM Tris-HCl [pH 8.0], 1 mM EDTA). Sonication settings were determined empirically to generate 0.5- to 2.0-kb DNA fragments. After sonication, insoluble debris was removed by centrifugation and the extracts precleared with 100 μl 50% protein A-Sepharose slurry (Pharmacia) for 45 min at 4°C. Precleared cell extracts (0.9 ml) were incubated overnight with 10 μl Fur antiserum (9) in 1× radioimmunoprecipitation assay (RIPA) buffer (140 mM NaCl, 10 mM Tris-HCl [pH 8.0], 1 mM EDTA, 1% Triton X-100, 0.1% SDS, 0.1% Na deoxycholate) at 4°C, and Fur-DNA complexes were immunoprecipitated with 50 μl 50% protein A slurry (preequilibrated in 1× RIPA buffer) for 3 h at 4°C in sterile disposable minicolumns (Bio-Rad). After the columns were drained by gravity flow, retained complexes were washed four times in 1× RIPA buffer, once in LiCl buffer (250 mM LiCl, 10 mM Tris-HCl [pH 8.0], 1 mM EDTA, 0.5% NP-40 [Igepal], 0.5% Na deoxycholate), and twice in TE, each for 10 min at 4°C under gentle agitation, and resuspended in 100 μl TE. DNA was recovered by treatment for 30 min at 37°C with RNase A (20 μg/ml) and overnight digestion with 50 μg/ml proteinase K in 0.5% SDS at 37°C. Cross-linking was reverted for 6 h at 65°C, with occasional mixing. DNA was extracted once with phenol-chloroform, back extracted with TE, and further extracted with chloroform. After the addition of 1% glycogen, DNA was ethanol precipitated and resuspended in 100 μl double-distilled H_2O. Immunoprecipitations with the *fur* deletion mutant and without Fur antiserum were routinely conducted as negative controls (control-IPs). To test the methodology, equal amounts of Fur-IP pools, column flowthrough, and controls were blotted on Hybond N+ nylon membranes (Pharmacia) with a Bio-Rad dot blot device and probed with promoter and coding regions of selected *H. pylori* genes labeled with an ECL nucleic acid labeling kit (Pharmacia). Probes for P_{frpB1}, P_{fecA2}, and an open reading frame (ORF) in the *fecA2* coding region located ca. 1,000 bp downstream of P_{fecA2} (ORF_{fecA2}) were generated by PCR with, respectively, oligonucleotides 875-F (cccgaattCCGTAATCACATTGTTG TCATCC) and 875-R (gggttctgcAGTAGGGGGAAACATAAAGCG) (7), A2F (tttaggatccTTTTGCTCAGTGGTTGTCAC) and A2R (tatagaattcGACGCTGG TTTTGCGATAGC), and CA2F (aattggatccTAAAACTCACTTGGTTGTTA) and CA2R (gtttgaattcCAGGAACTTCACTCAATAAT) (lowercase letters denote nucleotides added for cloning purposes).

Genome-wide location analyses. To map genomic binding sites, Fur-IP DNA pools (10 μl) were denatured at 94°C for 5 min in a thermal cycler and annealed to 100 pmol random hexamers (Promega). Probes were generated by incorporation of [α-^{33}P]dATP (Amersham) in two subsequent 45-min reactions using 5 U Klenow polymerase (New England BioLabs). Unincorporated radioactivity was removed by use of G-50 spin columns, and the labeled pool of probes was hybridized with *H. pylori* Panorama ORF macroarrays (Sigma-Genosys) by following the instructions of the manufacturer. Images were acquired with a Storm phosphorimager (Molecular Dynamics).

Transcriptome analyses. Total RNA was extracted from cells of both wild-type G27 and Δ*fur* strains grown to an OD_{600} of 0.6 and to an OD_{600} of 1.1, with and without iron/chelator treatment (Fe^+/Fe^-), by following a hot-phenol extraction procedure for *E. coli* microarrays (http://derisilab.ucsf.edu/microarray/pdfs/Total _RNA_from_Ecoli.pdf). Prior to reverse transcription, RNAs were treated with 1 U/μg RQ1 RNase-free DNase (Promega) at 37°C for 30 min, phenol-chloroform extracted, and ethanol precipitated. Integrity of the DNA-free RNA was assessed on 1% agarose gels prior to cDNA synthesis and labeling carried out in a thermal cycler (Roche). Twenty-five to 50 μg RNA was mixed with ca. 150 pmol random hexamers (Invitrogen) for 30-μl reactions, denatured for 3 min at 94°C, and annealed for 5 min at 37°C. Then, 20 μl of reverse transcriptase labeling mix (25 U avian myeloblastosis virus reverse transcriptase [Promega], 40 μCi [α-^{33}P]dATP, 80 U RNase inhibitor RNasin [Promega]) was added, and reverse transcription was allowed to proceed for 3 h. The reaction was stopped by the addition of 2 μl 0.5 M EDTA, and RNA was degraded by alkaline treatment with 0.15 N NaOH for 15 min at 37°C and thereafter neutralized with 17.5 μl 1 M Tris-HCl (pH 7.5). cDNA was purified from unincorporated label by use of Chromaspin-TE spin columns (Clontech) and hybridized to *H. pylori* Panorama ORF arrays (Sigma-Genosys) according to the manufacturer's instructions. Each experiment was originated from at least two biological replicates, and each replica was hybridized twice on the arrays. Images were acquired with a Storm phosphorimager (Molecular Dynamics).

Data analysis. Spot intensities on transcriptome and IP arrays were quantified with ImageQuant 5.2 software (Molecular Dynamics) and further processed with Microsoft Excel. The mean value of the 10 gene-specific spots with the lowest signal intensities, including the *fur* spot (HP1027) in the Δ*fur* arrays, was used to set the background level, which was subtracted from the remaining 1,671 spots. Spot signals were expressed as percent intensity with respect to the sum of all signal strengths above background levels on each array, and spots with percent intensity below 0.01 were not considered for subsequent analyses. For Fur-IPs, the absence of bias towards the identification of longer ORFs was established by best-fit linear regression analysis of the signal intensities of each spot plotted against the length of the spotted PCR product ($y = -2 \times 10^{-7} + 0.07$ and $y = -3 \times 10^{-6} + 0.06$ for iron-treated and iron-chelated Fur-IPs, respectively). Reproducibility of the immunoprecipitation experiment was assessed using percentile ranks. First, the Δ*fur* control-IP/genomic DNA and Fur-IP/genomic DNA raw signal ratios were calculated for each repetition. Thereafter, raw ratios were converted to percentile ranks and the data sets analyzed by mean percentile rank distribution. The mean ranks of control-IPs exhibited a normal distribution centered around the 50th percentile. On the contrary, the Fur-IP experiments (both Fe^+ and Fe^-) showed an overall uniform mean rank distribution above the 35th percentile, suggesting that for 934 gene targets immunoprecipitation is reproducible and Fur dependent. Statistically significant differences ($P < 0.05$) between control- and Fur-IP sets were assessed with a one-tailed Mann-Whitney test, as described by Laub et al. (20), and outliers were excluded from further analysis. Subsequently, unpaired enrichment values were calculated to estimate mean levels between Fur-IP and genomic input DNA sets (relative enrichment ratio), both for iron-treated and for iron-chelated cultures. For the analysis of iron-dependent enrichment (*n*-fold), or Fe ratio [(Fur-IP Fe^+)/(Fur-IP Fe^-)], unpaired IP values within iron-treated (Fe^+) and iron-chelated (Fe^-) Fur-IP sets were calculated. Statistical significance of relative enrichment and Fe ratios was determined by running the web-based Cyber-T application program (http://visitor.ics.uci.edu/genex/cybert) (19). Parameters for the estimation of the Bayesian standard deviation were chosen according to the settings suggested by the authors. Given our sample size of 1,671 genes, we adjusted the sliding window size to 81 and determined a Bayesian confidence estimate value corresponding to three times the number of experimental replicates. Genes with a relative enrichment ratio above 1.5 and a Bayesian *P* value of ≤0.01 were considered specific Fur targets. Genes with an Fe ratio of ≥±1.7 and a Bayesian *P* value of ≤0.01 were judged to be targeted by Fur in an iron-dependent fashion. Genes and targets not matching these criteria were not considered for further analysis, unless specified otherwise. Reproducibility of the Fe ratio was confirmed by best-fit linear regression analysis ($R^2 = 0.8258$). For transcriptome analyses, we first assayed the statistical significance of changed RNA accumulation in the *fur* mutant strain at an OD of 0.6 and at an OD of 1.1 by using Cyber-T (Δ*fur*/wt ≥ ±1.5; Bayesian *P* value ≤ 0.001). Genes with significant Δ*fur*/wt ratios

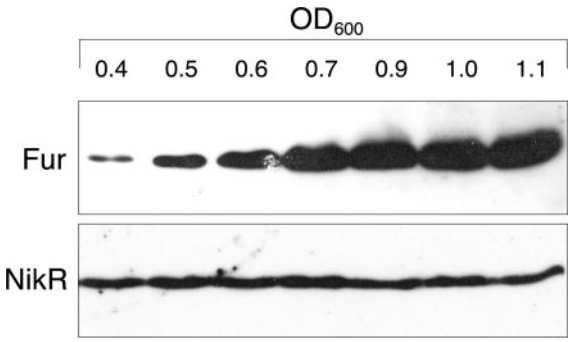

FIG. 1. Immunoblot of *H. pylori* protein extracts harvested at different growth stages (OD_{600} of 0.4 to OD_{600} of 1.1). Total protein extracts were loaded, and polypeptides were separated on a 15% SDS-PAGE gel. After blotting, the membrane was assayed with Fur and NikR antisera (1:3,000 and 1:1,000, respectively).

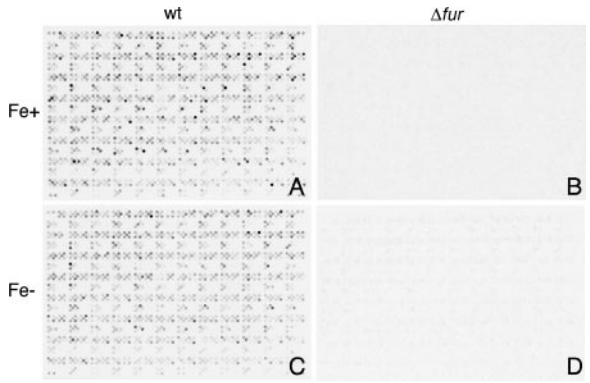

FIG. 2. Fur-IP macroarrays. *H. pylori* ORF macroarrays hybridized with Fur-immunoprecipitated DNA pools radioactively labeled by random hexamer extension using Klenow polymerase. Fur-IP in wild-type strain (A) and control Δ*fur* strain (B) after iron treatment (Fe^+) and in wild-type strain (C) and control Δ*fur* strain (D) after iron chelation (Fe^-). Note the decrease of signal intensity at specific spots upon iron chelation in the wild-type strain and the absence of detectable signals on Δ*fur* control arrays.

in only one of the two growth stages (*fur*- and phase-dependent transcripts) were further considered only if a consistent differential transcript variation between the growth phases (OD of 1.1/OD of 0.6 ratio; $P \leq 0.001$) could be ascertained between the mutant strain and the wild type. Parameters for the Bayesian standard deviation were set as described above.

Primer extensions. Primer extension analyses were performed at least twice with independent RNA preparations by using the oligonucleotides PE1432 (GTGGTG GTGTTGGCTGTTAGC) and *fla* (GCATGAGAAGTTAAAGCGGC) (30), as previously described (10).

RESULTS

Fur levels increase during growth. To optimize Fur-IPs, levels of the Fur protein were monitored during growth. Aliquots of the same *H. pylori* culture were harvested at regular time intervals, and total protein extracts were fractionated by SDS-PAGE and analyzed by immunoblotting with Fur antiserum; levels of the NikR regulator (6) were tested as a control. Interestingly, Fur accumulates in the cell during growth, while NikR levels remain constant (Fig. 1). These results defined the optimal OD range (0.7 to 1.1) at which the cultures had to be harvested to perform efficient Fur-IPs. They also showed distinct protein levels between Fur and NikR as a function of growth phase, which may influence transcription regulation of coregulated genes, especially those containing consecutive or overlapping Fur and NikR operators (6).

Identification of in vivo genomic Fur targets. To identify the whole set of genes directly targeted by the Fur protein, we implemented genome-wide location analyses, hybridizing Fur-IP DNA pools to *H. pylori* macroarrays. Bacterial cultures grown to an OD of 0.8 to 1.1 were exposed for 15 min to iron (Fe^+) or to the iron chelator 2,2′-dipyridyl (Fe^-) and in vivo cross-linked with formaldehyde. After sonication, protein-DNA complexes were immunoprecipitated with a nonsaturating amount of polyclonal Fur antiserum. Control-IPs were carried out in parallel with an isogenic Δ*fur* mutant (*fur*::*km*) and without antiserum. IP DNA pools to be used in location analysis are commonly labeled by (linker) PCR amplification prior to hybridization to DNA arrays. Pilot experiments revealed that efficient labeling of Fur-IP pools could be achieved using Klenow polymerase in random hexamer extensions, thereby retaining even slight differences in relative enrichment of immunoprecipitated DNA fragments (data not shown). Labeled IP DNA pools were hybridized to ORF macroarrays, manufactured with PCR products encompassing *H. pylori* 26695 and J99 coding sequences but not intergenic regions containing the promoters. The latter have an average size of ca. 175 bp in *H. pylori*, while sonicated Fur-IP DNA fragments used in our analyses were in the range of 0.5 to 2.0 kb. Therefore, immunoprecipitated binding sites encompassing a promoter likely extend into the coding region of the flanking genes.

ORF arrays probed with wild-type Fur-IP pools treated with iron revealed hundreds of spot signals with remarkable variations in intensity (Fig. 2A), while arrays probed with IP pools obtained in the Δ*fur* mutant strain failed to reveal significant signals (Fig. 2B). Iron chelation resulted in spot-specific reductions of the hybridization signal in the wild-type strain (Fig. 2C), while the amount of immunoprecipitated fragments hybridized on the control array resulted again in negligible signals (Fig. 2D). Triplicate independent Fur-IP and Δ*fur* control-IP experiments (from both iron-treated [Fe^+] and -chelated [Fe^-] cultures) were performed, and spot intensities on the arrays were quantified with a phosphorimager and analyzed as detailed in Materials and Methods. Reproducibility and statistical significance of relative enrichment levels between Fur-IP and genomic input DNA were analyzed, and spots exhibiting high enrichment reproducibility ($P \leq 0.01$) were assumed to be specific Fur targets. Furthermore, the iron-dependent enrichment (*n*-fold) for each target was calculated by dividing the IP values obtained after iron treatment by those obtained after chelation [(Fur-IP Fe^+)/(Fur-IP Fe^-), or Fe ratio].

Figure 3 shows a schematic representation of the results. The number of ORFs with significant relative enrichment (Fur-IP/input genomic DNA, $P \leq 0.01$) was 175 or 152 in cells treated with iron (Fig. 3A) or chelator (Fig. 3B), respectively. While 83 ORFs were common to both conditions, 92 were specific to iron and 69 to chelator. Furthermore, Fe ratio analysis showed a $\geq \pm 1.7$-fold iron-dependent enrichment ($P \leq 0.01$) at 85 ORFs (Fig. 3C), 18 of which were not iden-

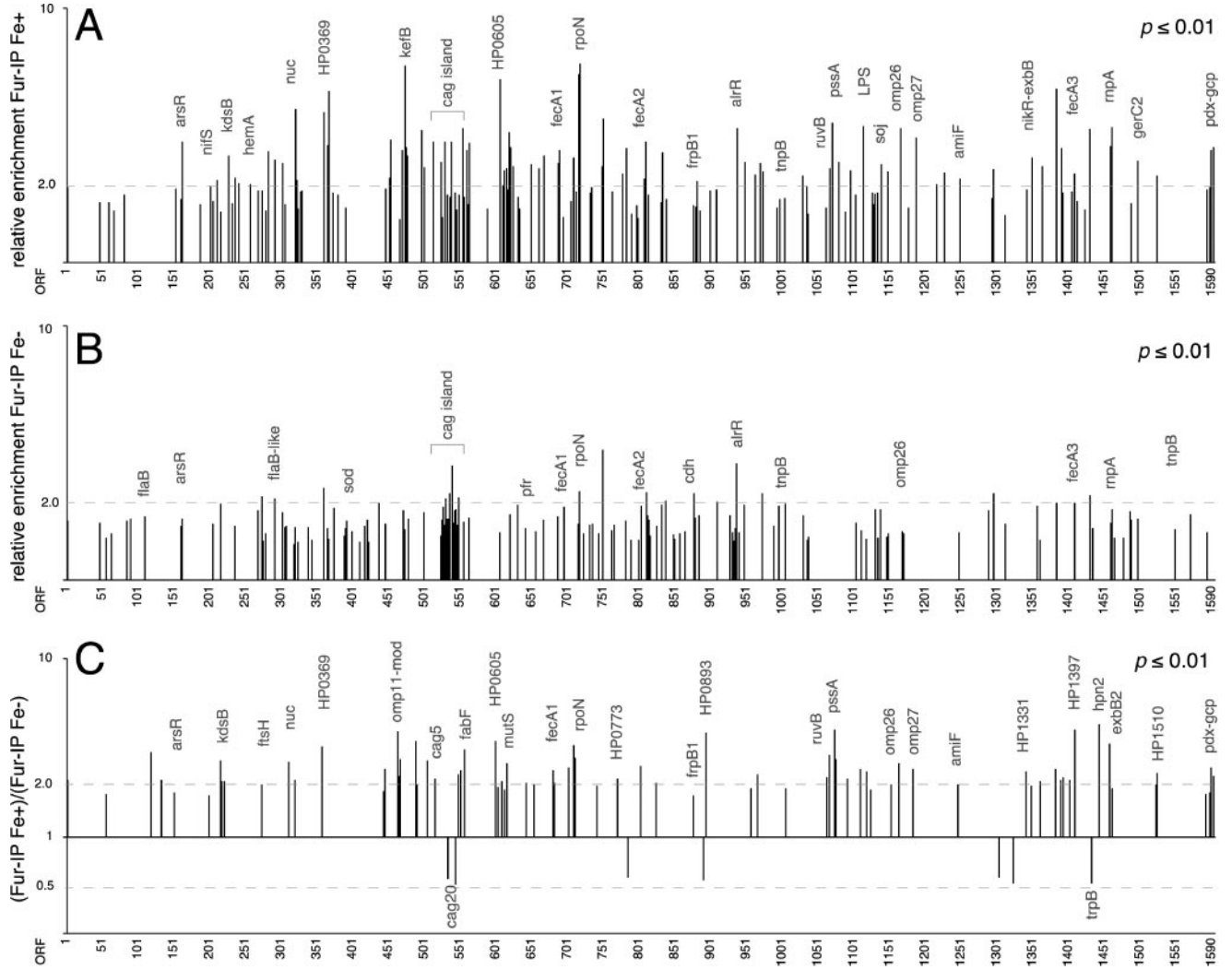

FIG. 3. Fur genome-wide location analysis. Fur-IP results plotted in log scale against the ordered series of *H. pylori* 26695 ORFs. Results are averages of three independent IP experiments. Dashed lines indicate the ±2.0 mark. (A) Genome-wide location analysis after iron treatment. Spikes denote relative enrichment levels of gene-specific Fur-IP Fe^+ signals compared to those for genomic input DNA. Note a group of binding sites clustered within the *cag* pathogenicity island. (B) Genome-wide location analysis after chelator treatment. Significant enrichment of gene-specific Fur-IP Fe^- signals is shown. (C) Iron-dependent Fur binding sites. The values of Fe ratios [(Fur-IP Fe^+)/(Fur-IP Fe^-)] are plotted. Spikes denote gene targets for which the enrichment levels of Fur-IP fragments significantly vary according to iron treatment ($P \leq 0.01$). Note the great majority of targets ($n = 78$) with an increased Fe ratio upon iron treatment (positive Fe ratios). Negative Fe ratios denote seven gene targets for which Fur binding augments upon iron chelation (note the absence of Fe ratios of < -2.0). Designations of representative genes are indicated.

tified above. As expected, the analysis predicts a Fur binding site upstream of genes known to be regulated by Fur, such as *frpB1*, *pfr*, *fecA1*, *fecA2*, and *fur* (Fig. 3) (9, 10, 32); therefore, these data do correlate with known Fur regulation.

Specific iron-dependent immunoprecipitation of Fur regulatory elements. To investigate whether Fur-IP signals on the ORF arrays reflect in vivo Fur-DNA interactions important for transcriptional regulation, an additional set of experiments was carried out. Fur-IP DNA pools as well as the column flowthrough and control-IPs (see Materials and Methods) were spotted on nylon membranes and probed with selected *H. pylori* promoter and coding regions (Fig. 4 and data not shown). The *frpB1* (HP0876) and *fecA2* (HP0807) genes, coding for an iron-regulated outer membrane protein and an iron dicitrate transport protein, respectively, are shown because transcription of both is modulated by Fur, mediated by binding of the regulator to iron-dependent operators in the case of the *frpB1* promoter, P_{frpB1} (7, 32).

After iron treatment and immunoprecipitation, P_{frpB1} is enriched approximately three- to fivefold compared to levels reached under iron-chelating conditions (Fig. 4A). This result is consistent with the iron-dependent affinity variation reported by use of Fur footprinting experiments performed in vitro with the same promoter fragment (10) and validated by the absence of detectable P_{frpB1} traces in control-IPs. The same blot was subsequently probed with a fragment encompassing the *fecA2* promoter (P_{fecA2}). Enrichment of P_{fecA2} is specific and Fur dependent (Fig. 4B); in this case, however, loss of enrichment in response to iron chelation is less pronounced than for P_{frpB1}. The blot was also hybridized with a probe corresponding to

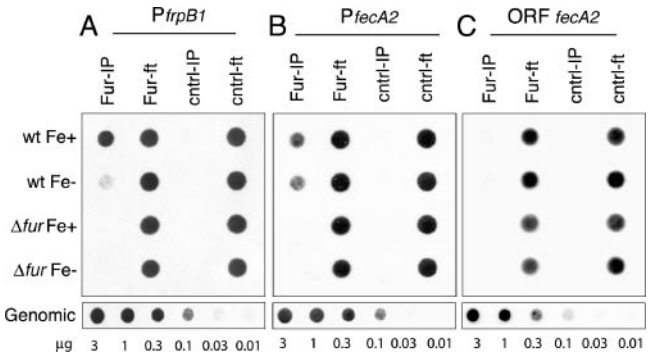

FIG. 4. Selective immunoprecipitation of genomic Fur targets. Dot blots of immunoprecipitated DNA from wt and Δ*fur H. pylori* cultures treated with iron (Fe^{+}) or chelator (Fe^{-}), hybridized with probes encompassing the *frpB1* promoter (A), the *fecA2* (HP0807) promoter (B), or a fragment of the *fecA2* coding region 1 kb downstream of the promoter (C). Fur-IP, IP with Fur antiserum; Fur-ft, column flowthrough of Fur-IP; cntrl-IP, control-IP without antiserum; cntrl-ft, column flowthrough of control-IP. Dilutions of genomic DNA (abscissa) were spotted as controls to visualize the relative enrichment levels of IP products.

ORF_{fecA2}. This probe displayed significantly weaker signals than the probe for P_{fecA2} (Fig. 4C), indicating that the Fur-bound elements are thus not likely to extend much more than 1,000 bp from the operator sequence. This observation has important consequences for the correct numbering of the genomic loci bound by Fur in vivo (see below).

Notably, the different effects of iron in dictating the efficiency of Fur binding to the *frpB1* and *fecA2* promoter regions (compare Fig. 4A and B) are reflected in dissimilar Fe ratios determined by the Fur-IP arrays. In fact, the *frpB1*-specific fragments are enriched 1.7-fold after iron treatment ($P < 0.01$), while *fecA2* enrichment is not significant ($P = 0.98$) (Fig. 3C). Based on this observation, it can be assumed that regulatory elements of Fur are specifically immunoprecipitated and identified in genome-wide location analyses using random primer labeling and ORF arrays.

Inter- and intracistronic Fur binding sites. A careful positional analysis of the distribution of Fur targets revealed that several mapped to consecutive ORFs. As this may arise from the immunoprecipitation of fragments of different lengths spanning a Fur binding site that could map to flanking ORFs, we considered clusters of targeted ORFs spanning less than 1,000 bp to represent a unique locus bound by Fur. With this assumption, we defined a total of 200 loci targeted by Fur (see Table S1A in the supplemental material). As a control, in vitro binding to several of the latter loci was confirmed by DNase I footprinting using purified Fur protein (data not shown). The majority of targeted loci ($n = 119$) map to ORFs adjacent to an intergenic region, where Fur regulatory control may be exerted at the promoter level, whereas the remaining 71 map within hypothetical polycistronic operons, >1,000 bp away from an intergenic region, or between two converging ORFs.

Because transcriptional control could occur within or immediately downstream from an identified Fur binding locus, transcriptome analyses were implemented to investigate which Fur loci were associated with iron-dependent Fur regulation.

Reconstruction of the *H. pylori* Fur regulon. Recently, several genes were reported to be influenced by the growth phase of the bacterium (25). Based on in silico identification of AT-rich boxes in their promoter regions, these were proposed to be under the control of Fur. Therefore, to take into consideration possible effects of the growth phase, Fur transcriptome analyses were carried out with labeled cDNAs from the wild type and the Δ*fur* strain treated with iron for 15 min either at an OD of 0.6 or at an OD of 1.1. Iron was added to minimize phase-dependent effects of iron depletion in the medium between an OD of 0.6 and an OD of 1.1 and to measure Fur-dependent transcriptional control shortly after the iron stimulus (10) rather than the long-term adaptation to iron or to the side effects of the *fur* deletion, associated with anomalous intracellular iron concentrations as observed with *E. coli* (24).

Data sets, assayed for statistical significance ($P \leq 0.001$) as described in Materials and Methods, revealed that the *fur* mutation affects mRNA abundance of 26 genes at an OD of 0.6 and 90 genes at an OD of 1.1. Differential expression values for genes deregulated in one or both of the growth phases were plotted on a two-dimensional scatter graph (Fig. 5A), which shows that the extent of *fur*-dependent regulation increases with growth (OD of 1.1), while the intensity of regulation is not very pronounced for many of those genes that change substantially at an OD of 1.1 (Fig. 5A). This could possibly reflect augmented transcriptional control of promoters with weak Fur operators, due to increased intracellular concentration of the regulator at the later growth phase (Fig. 1), but may also arise from indirect effects of the *fur* mutation in this phase.

To discriminate between direct regulation and indirect effects of the *fur* mutation, we compared the transcriptomes with the Fur-IP data sets, identifying the genes that are deregulated in the *fur* mutant and directly targeted in vivo by the Fur protein. This allowed us to pinpoint 59 genes, depicted in the scatter graph shown in Fig. 5B, which are direct targets of Fur and define the *H. pylori* Fur regulon (see Table S1B in the supplemental material). Moreover, 33 genes that are deregulated at an OD of 1.1 and are not targeted by the protein disappear from the graph (Fig. 5B), indicating that the effect of Fur on their regulation is indirect.

The *H. pylori* Fur regulon includes positively and negatively regulated genes. The Fur regulon includes 34 genes (including *fur*) that are subject to repression and, interestingly, 25 genes for which Fur control appears to be positive, as they are also targeted by the protein. Moreover, the regulatory targets of Fur fall into two classes: (i) 46 genes whose associated Fur binding sites suggest regulation at the promoter level and (ii) 13 genes, embedded within hypothetical operons, whose regulation appears to depend upon a nearby Fur binding site. The most important findings are reported below.

Overall, five main functional categories are subject to direct transcriptional control (Fig. 5C). The Fur regulon comprises 10 genes encoding metal transport and metal-binding proteins, including three iron dicitrate transporter *fecA* paralogs (HP0686, HP0807, and HP1400), *pfr* ferritin (HP0653), the *tonB* operon (HP1340-HP1341), *hpn2* (HP1432), and others, all of which are under negative regulatory control. Interestingly, two of these genes, *fecD* and *yaeE*, encoding transporter permeases, appear to be regulated from intracistronic positions. A few genes encoding metalloproteins involved in energy metabolism, such as the ATP

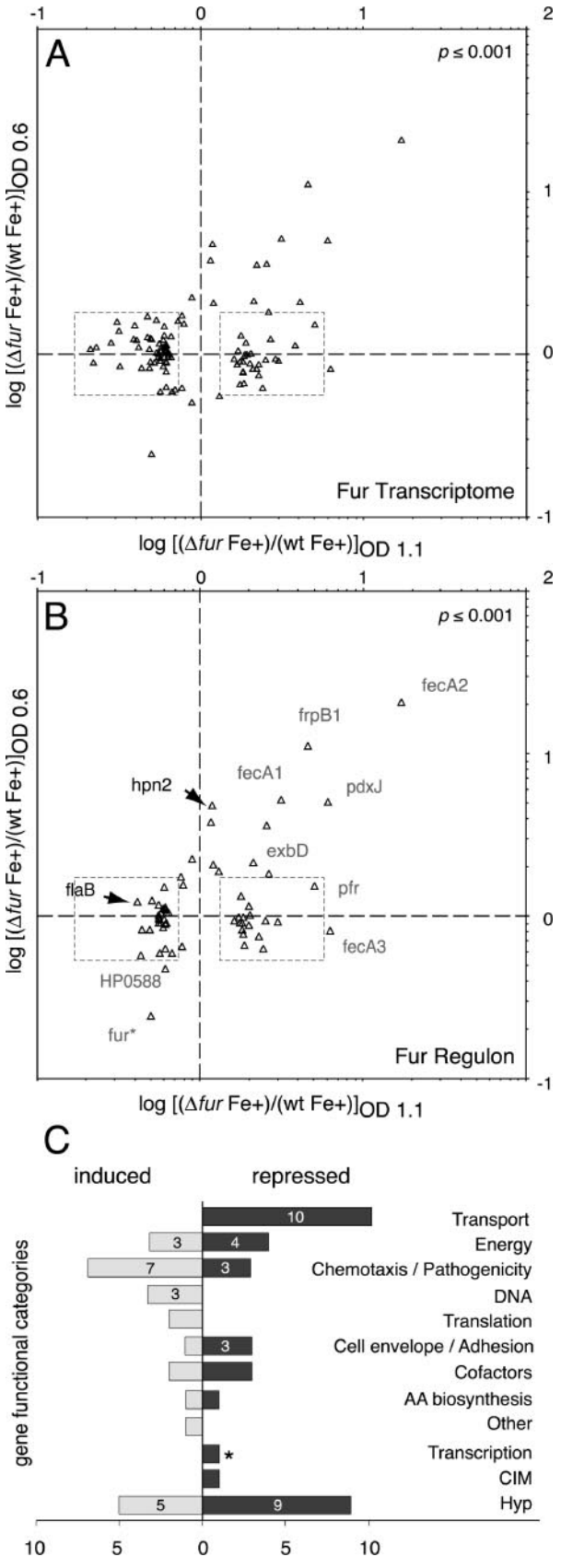

FIG. 5. Identification of the Fur regulon. (A) Fur transcriptome; log value of gene-specific deregulation due to *fur* mutation at an OD of 0.6 plotted against data at an OD of 1.1. Genes with differences (*n*-fold) below ±1.5 and *P* values of >0.001 were not included in the analysis. Dashed boxes denote a set of genes that are affected by the *fur* mutation particularly in the advanced growth phase. (B) Fur regulon; genes regulated in Fur transcriptome analysis (shown in panel A) were confronted with in vivo Fur binding sites identified by genome-wide location analyses (Fig. 3). All of the genes that were missing a Fur-binding locus amenable for transcriptional control (i.e., at or immediately upstream from the deregulated ORF) were excluded. This results in a panel of 59 genes that are deregulated by *fur* deletion and targeted by the Fur protein in vivo; these genes represent the direct targets of Fur regulation. Note the significant reduction of *fur*- and growth phase-dependent genes in the dashed boxes, indicating the occurrence of indirect effects of the *fur* mutation on transcript abundance, especially at an OD of 1.1. Designations of representative genes are indicated. The asterisk denotes the autorepressed *fur* gene, which is artifactually downregulated due to its substitution with a kanamycin cassette in the *fur* mutant strain. Arrows indicate two opposingly regulated genes selected for additional transcriptional analyses. (C) Functional categories of Fur regulon members. Numbers of induced and repressed genes (abscissa) are reported as a function of gene categories (ordinate). Abbreviations of functions are defined as follows: transport, transport and binding proteins; energy, energy metabolism; chemotaxis/pathogenicity, motility, chemotaxis, and pathogenicity; DNA, DNA metabolism, modification, and transposition; translation, genes involved in protein translation; cell envelope/adhesion, genes coding for outer membrane proteins and adhesins; cofactors, biosynthesis of cofactors, prosthetic groups, and carriers (heme, etc.); AA biosynthesis, amino acid biosynthesis; transcription, transcriptional regulators; CIM, central intermediary metabolism; Hyp, hypothetical genes and/or unknown function.

synthase F_0 subunit α (*atpB*), are also subject to negative regulation, while the ferredoxin oxidoreductase operon (HP0588-HP0591) appears to be positively regulated. Several of the 40 genes involved in motility and chemotaxis, including HP0295, *fliY*, *flgK*, *cheA*, and the major flagellin gene *flaB*, are Fur dependent and positively regulated in most cases. Finally, Fur also regulates transcription of several genes which may be important for cell adhesion or host-pathogen interactions, encoding outer membrane proteins (*omp20*, *omp24*, and HP1175), a fibronectin/fibrinogen-binding protein (HP1392), and a sialoglycoprotease homologue (*gcp*, or HP1584), or promoting hemolytic activity in other bacteria (5), as well as two genes of the *cag* pathogenicity island (*cag3* and *cag24*).

Opposite regulation by Fur. Because negative as well as positive effects of Fur on messenger abundance were revealed by our analysis and because this phenomenon appeared to be partially influenced by growth, which was especially apparent at an OD of 1.1 (Fig. 5B), we selected the *hpn2* (HP1432) and *flaB* (HP0115) genes as opposite representative cases to study in detail transcription regulation by Fur, iron, and growth phase. Transcription was assessed by primer extensions with total RNA extracted from wild-type and Δ*fur* strains, grown to an OD of 0.6 or an OD of 1.1 and treated with iron or chelator (Fig. 6). Primer extensions at the P_{frpB1} promoter were performed in parallel as a control (data not shown).

The *hpn2* transcriptional start site was mapped 47 bp upstream of the translation start codon and is preceded by a putative −10 box (TATAAA), suggesting that *hpn2* is transcribed by the vegetative RNA polymerase. Figure 6A shows that P_{hpn2} is derepressed by iron chelation, while iron results in full repression. Significantly, *fur* deletion leads to marked tran-

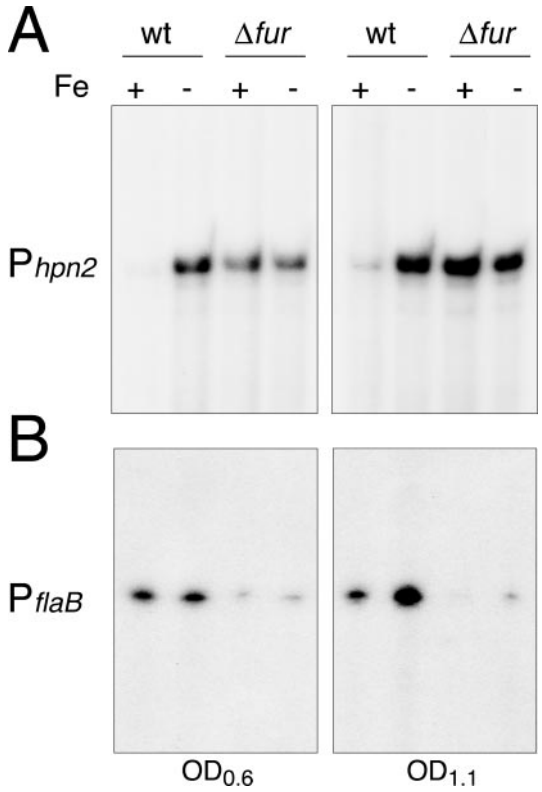

FIG. 6. Negative and positive transcriptional regulation of genes targeted by Fur. (A) Primer extension of the *hpn2* promoter with oligonucleotide PE1432 in wt and Δ*fur* strains 15 min after iron addition (Fe^+; 1 mM $FeSO_4$) or chelation (Fe^-; 100 μM 2,2′-dipyridyl). (B) Primer extension of the *flaB* promoter with oligonucleotide *fla* (30), showing marked transcriptional downregulation in *fur* mutants. Other details are as described for panel A.

scriptional derepression of the promoter, irrespective of iron treatment, indicating that *hpn2* is negatively regulated by Fur and iron. Moreover, the transcription from P_{hpn2} is derepressed in the *fur* mutant strain both at an OD of 0.6 and at an OD of 1.1.

Transcription of the *flaB* gene was previously shown to be under the control of a σ^{54}-dependent promoter, P_{flaB} (30). Interestingly, primer extensions performed with wild-type and *fur* mutant strains confirmed a marked reduction of transcription from P_{flaB} in the absence of Fur (Fig. 6B). Fur-dependent *flaB* regulation was found to be only marginally affected by the growth phase, although a slight increase of *flaB* mRNA levels could be detected upon iron chelation at an OD of 1.1. These results suggest a positive regulatory role of Fur on *flaB* transcription.

Together the results delineate the opposite effects of Fur-dependent transcriptional control and outline the complex regulatory circuit of this regulator, pointing to functions that extend beyond the classical repression paradigm.

DISCUSSION

Genome-wide location analysis has contributed significantly to the understanding of eukaryotic gene regulation, chromatin structure, and transcription factor binding to DNA and more recently has been applied to the dissection of bacterial regulatory circuits. In all of these cases, labeling of the immunoprecipitated DNA pools to be hybridized to the arrays was performed according to linker-mediated PCR protocols. This is a critical step because slight differences in the relative enrichment levels between target sequences can be lost during linker ligation and PCR amplification. To overcome this limitation, we successfully labeled *H. pylori* IP pools by using random hexamers and Klenow polymerase. Our results showed a very low level of background (Fig. 2) and significant reproducibility. To our knowledge, this is the first time that both the targets of a regulator protein (Fur) and the influence of a regulatory cofactor (iron) in governing protein-DNA interaction have been assessed in vivo at the genome-wide level. This may provide an improvement in the application of genome-wide location analyses of prokaryotes.

Extensive Fur binding in the *H. pylori* genome. The large number of identified binding sites indicates that Fur, like the *B. subtilis* SpoOA and the *Caulobacter crescentus* CtrA master regulators (20, 26), extensively binds to the *H. pylori* genome, supporting the hypothesis that Fur might function as a pleiotropic regulator. This behavior differs from that of other regulators that display a very restricted number of in vivo genomic targets, such as *E. coli* MelR, which targets solely the *melAB* promoter (17), and is in line with reports of other systems with abundant levels of Fur, estimated to have over 5,000 protein copies per cell (27). Possibly, Fur is persistently associated with specific DNA sequences in the *H. pylori* genome and binds to these sequences with distinct properties in an iron-dependent manner, reflecting accessibility and/or affinity variations of the protein for DNA. The observation that most (78/85) Fur targets have a positive Fe ratio (i.e., are more efficiently immunoprecipitated after iron treatment) (Fig. 3C) substantiates the hypothesis that Fur augments its affinity for many operators in the presence of the Fe cofactor.

Orphan Fur binding sites. The genes subjected to Fur regulatory control correspond to about a third of predicted Fur binding regions (59/200; 29.5%). This indicates the existence of a plethora of binding sites apparently not associated with iron regulation, which we call "orphan" binding sites. These binding sites map to both intergenic and intracistronic positions, raising questions about the functional significance of Fur binding at those sites. Recently, a genomic analysis of LexA binding revealed specific binding with operators not located to promoter regions of the *E. coli* genome, suggesting a permissive nature of the *E. coli* genome to transcription factor binding (34). Notably, the authors postulated high DNA binding specificity as well as selection against biologically irrelevant regions as general features of bacterial transcription factors. Accordingly, the orphan Fur binding sites are likely to represent specific targets for which novel regulatory or structural functions of Fur are yet to be discovered.

Comparison between Fur transcriptome analyses. Previous transcriptome analyses, studying the effects of iron starvation and growth phase, reported hundreds of genes affected by these conditions and possibly by Fur (25), while a more focused study, investigating the effect of *fur* mutation on cultures grown in iron-replete or -depleted media, recognized a restricted number of genes (12). Notably, the overlap between the Fur regulon members identified in our study and previous tran-

scriptome analyses is partial and basically limited to several iron uptake and trafficking genes. Although a number of regulatory targets may have been excluded because of the rather stringent statistical parameters used in macroarray data analysis, major differences may be attributable to the distinct experimental setup, which involves the analysis of protein binding and transcription levels shortly after the iron/chelator stimulus, in this study. Furthermore, we identified in vivo Fur binding at several genes previously reported to be influenced by iron concentration but not by the *fur* mutation. Examples include the *fliY* cistron, *fecA3*, *omp11*, *tnpB*, HP0806 (12), and several genes deregulated by iron starvation (25).

Positive regulation of Fur gene targets. An interesting observation of this study is that Fur sometimes appears to act as a positive regulator of transcription. This is particularly relevant for genes involved in motility and chemotaxis, like *flaB*, as these are essential for virulence, enabling colonization of the gastric mucosa. In agreement with a previous study (25), transcription of *flaB* is induced during iron starvation only in the advanced growth phase (Fig. 6B). As significant enrichment of *flaB* sequences was recorded in Fur-IP experiments (Fig. 3B), a direct role of Fur is expected at this promoter to function either as a direct activator of transcription, as reported for the *norB* gene in *Neisseria meningitidis* (8), or as a cofactor of the transcriptional apparatus. However, additional experiments will be needed to clarify the molecular mechanism of Fur positive regulation. Furthermore, despite the presence of Fur binding sites at *fur*-induced genes, the existence of small regulatory RNAs under Fur control should not be ruled out a priori (22, 35). Besides the mechanism of transcriptional induction exerted by Fur, the ability to sense iron and fine-tune expression of motility and chemotaxis genes could represent a critical aspect for successful colonization, as it would direct *H. pylori* to a suitable location for colonization. In support of this hypothesis is the finding that two genes of the *cag* pathogenicity island, which are important for *H. pylori* virulence, appear to be similarly regulated.

Intracistronic regulation. Genes within polycistronic operons, deregulated by the *fur* mutation and associated with Fur binding sites, may indicate the occurrence of intracistronic regulation. This intriguing finding certainly deserves further investigation in the future. Tentatively, it may be hypothesized that Fur occupies regulatory elements that control transcriptional initiation from promoters that map within the operon. Another possibility is that these intracistronic binding sites embody Fur regulatory elements downstream from the promoter. Similar elements were recently shown to affect the H-NS-dependent regulation of the *bgl* operon in *E. coli*, which is regulated at two levels: by a bent AT-rich H-NS operator upstream of the promoter down-regulating transcription and by a silencer region located ca. 600 bp downstream of the *bgl* transcriptional start site, which induces stalling of elongation and rho-dependent repression when H-NS is bound to it (11).

Dissection of the *H. pylori* metal regulatory circuit. By analogy to the PerR and Fur proteins of *B. subtilis*, two Fur family members that govern metal homeostasis (16), the *H. pylori* NikR and Fur proteins may be involved in overlapping regulatory loops. In fact, many genes deregulated by *nikR* mutation (4) are also regulated by Fur, but not necessarily with the same regulatory output. For example, both regulators repress the *tonB* operon, as well as the *pfr* and *fecA3* genes. By contrast, it appears that transcription of *flaB* is repressed by NikR (4) and activated by Fur (Fig. 6B), while transcription of the *hnp2* gene is repressed by Fur (Fig. 6A) and activated by NikR (4). It was proposed that NikR regulation of Fur-controlled genes is mediated by titration of free metal ions through transcriptional control of the TonB uptake system (4). However, from our analysis it can also be hypothesized that Fur regulation is mediated by direct protein-DNA interactions at genes that are regulated by NikR. Very recently, it was shown that the two regulators contact promoters with flanking and overlapping operators (6). This suggests a multifactorial net output of the metal regulatory circuit, influenced by metal (cofactor) concentration, regulator concentration, binding affinity, and relative positions of operators. Growth phase appears to play only a marginal role in transcriptional control, although it influences the relative protein concentrations of Fur. Clearly, the dissection of this circuit will benefit from additional studies investigating also the genomic targets of NikR and other regulators, which may influence metal trafficking and metalloenzyme activity and thereby *H. pylori* virulence.

ACKNOWLEDGMENTS

We thank F. Pezzetti and Fondazione Cassa di Risparmio in Bologna—Centro di Ricerca sulla Genetica and G. Capranico and Centro Interdipartimentale di Ricerche Biotecnologiche (CIRB) for use of the phosphorimager. We acknowledge the skillful contribution of F. Agriesti to the project and thank D. Diolaiti, A. Khobta, and G. Perini for fruitful discussions.

This work was supported partially by Chiron and by the University of Bologna (to V.S.).

REFERENCES

1. **Alm, R. A., L. S. Ling, D. T. Moir, B. L. King, E. D. Brown, P. C. Doig, D. R. Smith, B. Noonan, B. C. Guild, B. L. deJonge, G. Carmel, P. J. Tummino, A. Caruso, M. Uria-Nickelsen, D. M. Mills, C. Ives, R. Gibson, D. Merberg, S. D. Mills, Q. Jiang, D. E. Taylor, G. F. Vovis, and T. J. Trust.** 1999. Genomic-sequence comparison of two unrelated isolates of the human gastric pathogen *Helicobacter pylori*. Nature **397:**176–180.
2. **Baichoo, N., and J. D. Helmann.** 2002. Recognition of DNA by Fur: a reinterpretation of the Fur box consensus sequence. J. Bacteriol. **184:**5826–5832.
3. **Bury-Mone, S., J. M. Thiberge, M. Contreras, A. Maitournam, A. Labigne, and H. De Reuse.** 2004. Responsiveness to acidity via metal ion regulators mediates virulence in the gastric pathogen *Helicobacter pylori*. Mol. Microbiol. **53:**623–638.
4. **Contreras, M., J. M. Thiberge, M. A. Mandrand-Berthelot, and A. Labigne.** 2003. Characterization of the roles of NikR, a nickel-responsive pleiotropic autoregulator of *Helicobacter pylori*. Mol. Microbiol. **49:**947–963.
5. **Crasta, K. C., K.-L. Chua, S. Subramaniam, J. Frey, H. Loh, and H.-M. Tan.** 2002. Identification and characterization of CAMP cohemolysin as a potential virulence factor of *Riemerella anatipestifer*. J. Bacteriol. **184:**1932–1939.
6. **Delany, I., R. Ieva, A. Soragni, M. Hilleringman, R. Rappuoli, and V. Scarlato.** 2005. In vitro analysis of protein-operator interactions of the NikR and Fur metal-responsive regulators in overlapping sets of genes in *Helicobacter pylori*. J. Bacteriol. **187:**7703–7715.
7. **Delany, I., A. B. Pacheco, G. Spohn, R. Rappuoli, and V. Scarlato.** 2001. Iron-dependent transcription of the *frpB* gene of *Helicobacter pylori* is controlled by the Fur repressor protein. J. Bacteriol. **183:**4932–4937.
8. **Delany, I., R. Rappuoli, and V. Scarlato.** 2004. Fur functions as an activator and as a repressor of putative virulence genes in *Neisseria meningitidis*. Mol. Microbiol. **52:**1081–1090.
9. **Delany, I., G. Spohn, A. B. Pacheco, R. Ieva, C. Alaimo, R. Rappuoli, and V. Scarlato.** 2002. Autoregulation of *Helicobacter pylori* Fur revealed by functional analysis of the iron-binding site. Mol. Microbiol. **46:**1107–1122.
10. **Delany, I., G. Spohn, R. Rappuoli, and V. Scarlato.** 2001. The Fur repressor controls transcription of iron-activated and -repressed genes in *Helicobacter pylori*. Mol. Microbiol. **42:**1297–1309.
11. **Dole, S., V. Nagarajavel, and K. Schnetz.** 2004. The histone-like nucleoid structuring protein H-NS represses the *Escherichia coli bgl* operon downstream of the promoter. Mol. Microbiol. **52:**589–600.

12. **Ernst, F. D., S. Bereswill, B. Waidner, J. Stoof, U. Mader, J. G. Kusters, E. J. Kuipers, M. Kist, A. H. van Vliet, and G. Homuth.** 2005. Transcriptional profiling of *Helicobacter pylori* Fur- and iron-regulated gene expression. Microbiology **151:**533–546.
13. **Escolar, L., J. Perez-Martin, and V. de Lorenzo.** 1998. Binding of the *fur* (ferric uptake regulator) repressor of *Escherichia coli* to arrays of the GA TAAT sequence. J. Mol. Biol. **283:**537–547.
14. **Escolar, L., J. Perez-Martin, and V. de Lorenzo.** 1999. Opening the iron box: transcriptional metalloregulation by the Fur protein. J. Bacteriol. **181:**6223–6229.
15. **Fuangthong, M., and J. D. Helmann.** 2003. Recognition of DNA by three ferric uptake regulator (Fur) homologs in *Bacillus subtilis*. J. Bacteriol. **185:**6348–6357.
16. **Fuangthong, M., A. F. Herbig, N. Bsat, and J. D. Helmann.** 2002. Regulation of the *Bacillus subtilis fur* and *perR* genes by PerR: not all members of the PerR regulon are peroxide inducible. J. Bacteriol. **184:**3276–3286.
17. **Grainger, D. C., T. W. Overton, N. Reppas, J. T. Wade, E. Tamai, J. L. Hobman, C. Constantinidou, K. Struhl, G. Church, and S. J. Busby.** 2004. Genomic studies with *Escherichia coli* MelR protein: applications of chromatin immunoprecipitation and microarrays. J. Bacteriol. **186:**6938–6943.
18. **Hantke, K.** 2001. Iron and metal regulation in bacteria. Curr. Opin. Microbiol. **4:**172–177.
19. **Hatfield, G. W., S. P. Hung, and P. Baldi.** 2003. Differential analysis of DNA microarray gene expression data. Mol. Microbiol. **47:**871–877.
20. **Laub, M. T., S. L. Chen, L. Shapiro, and H. H. McAdams.** 2002. Genes directly controlled by CtrA, a master regulator of the *Caulobacter* cell cycle. Proc. Natl. Acad. Sci. USA **99:**4632–4637.
21. **Lee, H. W., Y. H. Choe, D. K. Kim, S. Y. Jung, and N. G. Lee.** 2004. Proteomic analysis of a ferric uptake regulator mutant of *Helicobacter pylori*: regulation of *Helicobacter pylori* gene expression by ferric uptake regulator and iron. Proteomics **4:**2014–2027.
22. **Massé, E., F. E. Escorcia, and S. Gottesman.** 2003. Coupled degradation of a small regulatory RNA and its mRNA targets in *Escherichia coli*. Genes Dev. **17:**2374–2383.
23. **Massé, E., and S. Gottesman.** 2002. A small RNA regulates the expression of genes involved in iron metabolism in *Escherichia coli*. Proc. Natl. Acad. Sci. USA **99:**4620–4625.
24. **McHugh, J. P., F. Rodriguez-Quinones, H. Abdul-Tehrani, D. A. Svistunenko, R. K. Poole, C. E. Cooper, and S. C. Andrews.** 2003. Global iron-dependent gene regulation in *Escherichia coli*. A new mechanism for iron homeostasis. J. Biol. Chem. **278:**29478–29486.
25. **Merrell, D. S., L. J. Thompson, C. C. Kim, H. Mitchell, L. S. Tompkins, A. Lee, and S. Falkow.** 2003. Growth phase-dependent response of *Helicobacter pylori* to iron starvation. Infect. Immun. **71:**6510–6525.
26. **Molle, V., M. Fujita, S. T. Jensen, P. Eichenberger, J. E. Gonzalez-Pastor, J. S. Liu, and R. Losick.** 2003. The SpoOA regulon of *Bacillus subtilis*. Mol. Microbiol. **50:**1683–1701.
27. **Ochsner, U. A., A. I. Vasil, Z. Johnson, and M. L. Vasil.** 1999. *Pseudomonas aeruginosa fur* overlaps with a gene encoding a novel outer membrane lipoprotein, OmlA. J. Bacteriol. **181:**1099–1109.
28. **Pflock, M., S. Kennard, I. Delany, V. Scarlato, and D. Beier.** 2005. Acid-induced activation of the urease promoters is mediated directly by the ArsRS two-component system of *Helicobacter pylori*. Infect. Immun. **73:**6437–6445.
29. **Ratledge, C., and L. G. Dover.** 2000. Iron metabolism in pathogenic bacteria. Annu. Rev. Microbiol. **54:**881–941.
30. **Spohn, G., and V. Scarlato.** 1999. Motility of *Helicobacter pylori* is coordinately regulated by the transcriptional activator FlgR, an NtrC homolog. J. Bacteriol. **181:**593–599.
31. **Tomb, J. F., O. White, A. R. Kerlavage, R. A. Clayton, G. G. Sutton, R. D. Fleischmann, K. A. Ketchum, H. P. Klenk, S. Gill, B. A. Dougherty, K. Nelson, J. Quackenbush, L. Zhou, E. F. Kirkness, S. Peterson, B. Loftus, D. Richardson, R. Dodson, H. G. Khalak, A. Glodek, K. McKenney, L. M. Fitzegerald, N. Lee, M. D. Adams, J. C. Venter, et al.** 1997. The complete genome sequence of the gastric pathogen *Helicobacter pylori*. Nature **388:**539–547.
32. **van Vliet, A. H., J. Stoof, R. Vlasblom, S. A. Wainwright, N. J. Hughes, D. J. Kelly, S. Bereswill, J. J. Bijlsma, T. Hoogenboezem, C. M. Vandenbroucke-Grauls, M. Kist, E. J. Kuipers, and J. G. Kusters.** 2002. The role of the ferric uptake regulator (Fur) in regulation of *Helicobacter pylori* iron uptake. Helicobacter **7:**237–244.
33. **Vasil, M. L., and U. A. Ochsner.** 1999. The response of *Pseudomonas aeruginosa* to iron: genetics, biochemistry and virulence. Mol. Microbiol. **34:**399–413.
34. **Wade, J. T., N. B. Reppas, G. M. Church, and K. Struhl.** 2005. Genomic analysis of LexA binding reveals the permissive nature of the *Escherichia coli* genome and identifies unconventional target sites. Genes Dev. **19:**2619–2630.
35. **Wilderman, P. J., N. A. Sowa, D. J. FitzGerald, P. C. FitzGerald, S. Gottesman, U. A. Ochsner, and M. L. Vasil.** 2004. Identification of tandem duplicate regulatory small RNAs in *Pseudomonas aeruginosa* involved in iron homeostasis. Proc. Natl. Acad. Sci. USA **101:**9792–9797.